Anisotropic Colossal Magnetoresistance Effects in Fe$_{1-x}$Cu$_x$Cr$_2$S$_4$

V. Fritsch[1], J. Deisenhofer[1], R. Fichtl[1], J. Hemberger[1], H.-A. Krug von Nidda[1], M. Mücksch[2],
M. Nicklas[3], D. Samusi[4], J. D. Thompson[3], R. Tidecks[2], V. Tsurkan[2,4], A. Loidl[1]

[1]*Experimentalphysik V, Elektronische Korrelationen und Magnetismus,*
Institut für Physik, Universität Augsburg, D-86135 Augsburg
[2]*Institut für Physik, Universität Augsburg, D-86135 Augsburg*
[3]*Los Alamos National Laboratory, Los Alamos, NM 87545, USA*
[4]*Institute of Applied Physics, Academy of Science of Moldova, Academiei 5, MD-2028, Chisinau*

A detailed study of the electronic transport and magnetic properties of Fe$_{1-x}$Cu$_x$Cr$_2$S$_4$ ($x \leq 0.5$) on single crystals is presented. The resistivity is investigated for $2 \leq T \leq 300$ K in magnetic fields up to 140 kOe and under hydrostatic pressure up to 16 kbar. In addition magnetization and ferromagnetic resonance (FMR) measurements were performed. FMR and magnetization data reveal a pronounced magnetic anisotropy, which develops below the Curie temperature, T_C, and increases strongly towards lower temperatures. Increasing the Cu concentration reduces this effect. At temperatures below 35 K the magnetoresistance, $MR = \frac{\rho(0)-\rho(H)}{\rho(0)}$, exhibits a strong dependence on the direction of the magnetic field, probably due to an enhanced anisotropy. Applying the field along the hard axis leads to a change of sign and a strong increase of the absolute value of the magnetoresistance. On the other hand the magnetoresistance remains positive down to lower temperatures, exhibiting a smeared out maximum with the magnetic field applied along the easy axis. The results are discussed in the ionic picture using a triple-exchange model for electron hopping as well as a half-metal utilizing a band picture.

PACS numbers: 75.30.Vn, 71.30.+h

I. INTRODUCTION

Manganites, especially LaMnO$_3$ and relatives, are known for their unusual transport and magnetic properties since more than 50 years.[1,2] However, the appreciation and intensive interest is a recent development, which started with the giant magnetoresistance (actually named colossal magnetoresistance, CMR) in thin films of La$_{2/3}$Ba$_{1/3}$MnO$_3$, published by von Helmolt *et al.* in 1993,[3] even though a negative magnetoresistance of nearly 20 % was discovered in bulk La$_{0.69}$Pb$_{0.31}$MnO$_3$ by Searle and Wang already in 1970.[4] Soon after the onset of the renewed interest in these materials, it was realized that the theoretical framework used in the past to understand the manganites' behaviour does not survive a quantitative analysis.[5,6] The complexity of the problem led to the perception that manganites are prototypical for correlated electron systems, where spin, charge and orbital degrees of freedom are strongly coupled. These couplings lead to a failure of the classical approach, which neglects some interactions for simplification, and opens the way for a complete range of new physics. As a consequence the experimental and theoretical studies of manganites and related compounds give the unique opportunity of getting a deeper understanding of the fundamental physics responsible for phenomena like colossal magnetoresistance or high-temperature superconductivity.

Looking for new materials exhibiting a CMR effect, the substitution of oxygen with the isoelectronic sulphur seems to be a promising way.[7] Magnetoresistance effects in some chalcogenide spinels were reported previously by Watanabe[8] and Ando[9]. An elaborately review about this

is given in Ref. 10. Since the CMR is associated with a double-exchange mechanism, the rediscovery of a CMR effect in the chalcospinel FeCr$_2$S$_4$,[11] which is neither oxide nor perovskite, opened a wide field for the further exploration and exploitation of magnetoresistance effects.

FeCr$_2$S$_4$ is a ferrimagnetic semiconductor, crystallizing in the normal spinel structure, where the Cr ions occupy the octahedral and the Fe ions the tetrahedral sites.[12] The Fe- and the Cr-sublattices are aligned antiparallel in the ferrimagnetic state. In single-crystalline FeCr$_2$S$_4$ the Curie temperature is $T_C = 167$ K and around T_C a negative magnetoresistance is observed.[11] Doping with nonmagnetic Cu on the Fe site, Fe$_{1-x}$Cu$_x$Cr$_2$S$_4$ ($x \leq 0.5$), shifts the Curie temperature upwards accompanied by a decreasing magnetoresistance without changing substantially the magnetic properties.[12]

Polycrystalline samples of Fe$_{1-x}$Cu$_x$Cr$_2$S$_4$ were first synthesized in the fifties and sixties of the last century.[13] To explain the physical properties two competing models with different valences of the involved ions were proposed. Lotgering *et al.*[14] developed a model considering a monovalent Cu$^+$-ion over the whole concentration range, while Goodenough[15] postulated divalent Cu^{2+} for the concentration range $0.5 < x \leq 1$. Furthermore the existence of monovalent S$^-$ was discussed at these times.[14]

Mößbauer-spectroscopy studies reveal divalent Fe^{2+} ions in FeCr$_2$S$_4$, but trivalent Fe^{3+} in Fe$_{0.5}$Cu$_{0.5}$Cr$_2$S$_4$.[16,17] X-ray photoelectron-spectroscopy measurements show that Cu is monovalent in Fe$_{0.5}$Cu$_{0.5}$Cr$_2$S$_4$ and in CuCr$_2$Se$_4$, which means it is in a $3d^{10}$ state[18]. NMR-measurements and bandstructure calculations lead to the same conclusion for the Cu valence in CuIr$_2$S$_4$.[19,20] All samples under

investigation in this study were prepared as described in Ref. 18 and found to contain only divalent S. Therefore Cu existing only in the non-magnetic $3d^{10}$ state and divalent S only is assumed. The later discussion adopts this assumption.

II. EXPERIMENTAL METHODS

Single crystals of Cu-substituted $FeCr_2S_4$ were grown by the chemical transport-reaction method from poly-crystalline material obtained by a solid-state reaction. In this paper samples with Cu-concentrations $x = 0.05$, 0.1, 0.2, 0.3, 0.4, and 0.5 are studied.

The X-ray diffraction measurements were performed with a Stoe X-ray diffractometer. Single crystals were powdered and diffraction spectra were taken from $35°$ to $130°$ and analyzed with the Visual X^{POW} software.

The magnetic properties were measured using a super-conducting quantum interference device (SQUID) mag-netometer (Quantum Design) in the temperature range $1.8 \leq T \leq 400$ K in external fields up to 70 kOe. In addition ferromagnetic (or better ferrimagnetic) resonance (FMR) measurements were carried out at X-band fre-quencies (9.4 GHz) with a Bruker ELEXSYS E500-CW spectrometer using a continuous Helium gas-flow cryostat (Oxford Instruments) for temperatures $4.2 \leq T \leq 300$ K. For the FMR experiments thin polished disks prepared in (110) plane orientation with about 1 mm diameter and 0.05 mm thickness were used.

The electrical resistivity was measured in an Oxford ^{4}He cryostat equipped with a superconducting magnet capable of magnetic fields up to 16 T. Conventional dc four-point techniques were used with currents between 0.5 and 500 μA at temperatures $2 \leq T \leq 300$ K. Gold wire with a diameter of 25 μm and silver paint were used to prepare the electrical contacts. The contact resistance was always between 20 and 70 Ω. To prevent problems occurring due to aging of the contacts, leading to a con-tact resistance several orders of magnitudes higher, the measurements were performed immediately after prepar-ing the contacts.

Hydrostatic pressure was produced in a conventional Be-Cu clamp type cell using fluorinert^{TM} as a pressure medium. The pressure at low temperatures was deter-mined from the shift of the inductively measured T_C of a small piece of lead, located in immediate proximity to the sample. The width of the superconducting transition of Pb did not exceed 15 mK, indicating good hydrostatic conditions and providing an estimate of the pressure-measurement uncertainty, ± 0.4 kbar. The pressure at room temperature was determined from the pressure de-pendence of the resistivity of a manganin wire placed inside the cell.
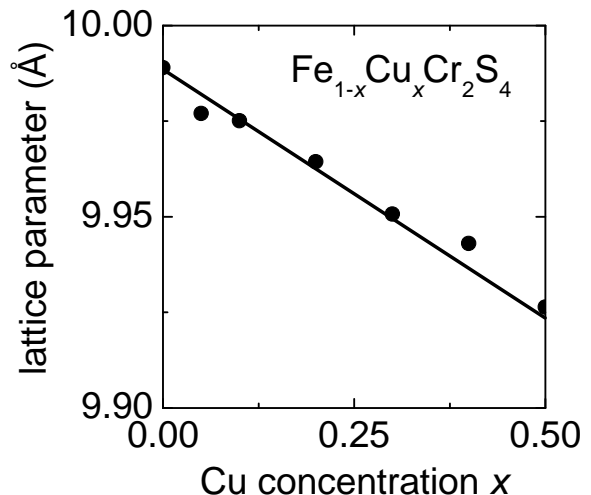

FIG. 1: Cubic lattice parameter vs Cu concentration x in $Fe_{1-x}Cu_xCr_2S_4$.

TABLE I: Curie temperature T_C of $Fe_{1-x}Cu_xCr_2S_4$, deter-mined by magnetization measurements, and electrical resis-tivity, ρ, at room temperature ($T = 290$ K) for specimens of different Cu concentrations, x.

x	T_C (K $\pm$ 0.5)	ρ(290 K) (mΩcm $\pm$10%)
0	167	236 (Ref. 21)
0.05	182	79.2
0.1	197	8.2
0.2	215	10.1
0.3	232	11.6
0.4	236	14.9
0.5	275	26.8

III. EXPERIMENTAL RESULTS

A. X-ray Diffraction

In $FeCr_2S_4$ the substitution of Fe by Cu leads to a linear dependence of the lattice parameter of the cubic spinel structure on the Cu concentration following Ve-gard's law, as shown in figure 1. In addition, the X-ray studies of powdered single crystals confirmed single-phase material with no detectable parasitic phases.

B. Magnetization

The Curie temperatures T_C of $Fe_{1-x}Cu_xCr_2S_4$ are listed in table I, as determined by the kink-point-method[22] from magnetization measurements, and the room temperature resistivity, which will be discussed in section IV B. The Curie temperature T_C increases with the Cu-concentration x. The same trend has been ob-
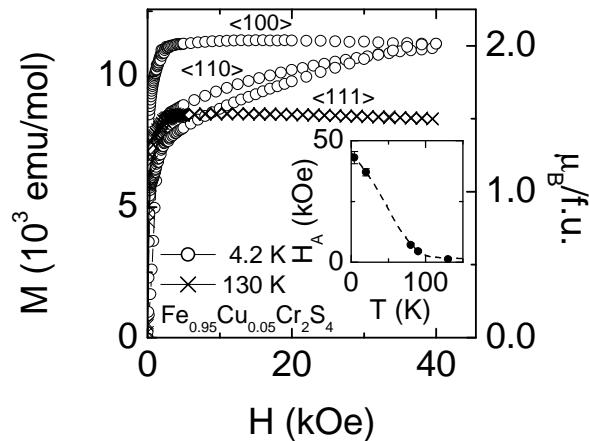
FIG. 2: Magnetization of $Fe_{0.95}Cu_{0.05}Cr_2S_4$ vs. magnetic field at $T = 4.2$ K ($\bigcirc$) and $T = 130$ K ($\times$, here all crystallographic orientations are nearly coincide) respectively. Inset: Anisotropy field H_A vs. temperature. The dashed line is to guide the eyes.

served for polycrystalline samples,[12] though for higher Cu concentrations T_C remains at a lower value in single crystals. Figure 2 shows the magnetization, M, for $Fe_{0.95}Cu_{0.05}Cr_2S_4$ versus the magnetic field, H, at $T = 4.2$ K and $T = 130$ K, respectively. At $T = 4.2$ K the magnetic anisotropy is clearly observed. For the easy magnetization axis $\langle 100 \rangle$ the saturation is already reached at 2 kOe whereas for the hard axis $\langle 111 \rangle$ and the intermediate axis $\langle 110 \rangle$ saturation only occurs at 43 kOe. The temperature dependence of the anisotropy field H_A, defined by the magnetic field where saturation is reached for all three directions, is shown in the inset of figure 2. It decreases monotonically with increasing temperature and vanishes at T_C.

C. FMR-Measurements

For a more detailed analysis of the magnetic anisotropy we performed ferromagnetic resonance (FMR) measurements, which will be published in a separate paper. Here we confine ourselves to the presentation of one illustrative result, which nicely reflects the evolution of the anisotropy with increasing Cu concentration and can be explained on the base of the FMR results published recently for $FeCr_2S_4$ single crystals.[23] For the samples under investigation ($0 < x \leq 0.5$) the FMR line exhibits an analogous behavior to the pure compound $x = 0$. Figure 3 shows the temperature dependence of the resonance field H_{res} for several Cu concentrations below the Curie temperature. The static magnetic field was applied along an $\langle 111 \rangle$ or $\langle 100 \rangle$ axis within the (110) plane of the disk-shaped samples and the magnetic microwave field was applied perpendicular to the plane. This geometry al-
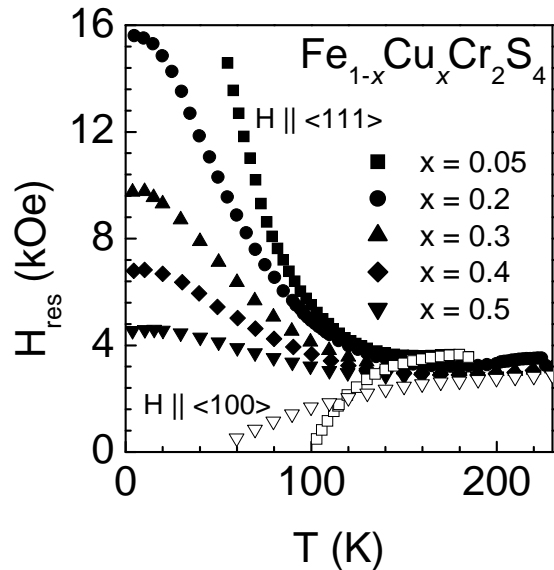

FIG. 3: Resonance field H_{res} of $Fe_{1-x}Cu_xCr_2S_4$ of the FMR spectrum as a function of the temperature for the magnetic field applied parallel to the hard axis $\langle 111 \rangle$ (closed symbols). Additionally the resonance field H_{res} for $x = 0.05$ and 0.5 with the magnetic field applied in the easy direction $\langle 100 \rangle$ are shown (open symbols). The anisotropy of H_{res} reflects the magnetocrystalline anisotropy in the system.

lows measurements at different orientations of the static field in the plane without change of the demagnetization contributions to the resonance condition.[24,25] Just below the Curie temperature the resonance field H_{res} is approximately isotropic given by the Larmor frequency $\nu = \gamma H_{res}$, with the microwave frequency ν and the gyromagnetic ratio γ determined by the g-values of the two sublattices.[26] With decreasing temperature one observes first a slight shift to smaller fields due to the demagnetization but then a strongly anisotropic behavior appears. For the magnetic field applied along the easy $\langle 100 \rangle$ axis, the resonance line shifts to low fields and disappears at a finite temperature as shown exemplarily for $x = 0.05$ and $x = 0.5$. For the field applied parallel to the hard $\langle 111 \rangle$ axis, the resonance field shifts to higher fields. A similar shift to higher fields is observed for orientation along the intermediate $\langle 110 \rangle$ axis (not shown in figure 3). The maximum shift at low temperatures decreases with increasing Cu concentration.

This result is directly related to the decrease of the magnetic anisotropy. Neglecting the demagnetization effects, which turn out to be small compared to the anisotropy field at low temperatures[23] and taking into account only the first-order cubic anisotropy field $H_A = K_1/M$, where K_1 is the first-order cubic anisotropy constant, the resonance conditions read for $\langle 100 \rangle$ and $\langle 111 \rangle$ orientation, respectively:[26]
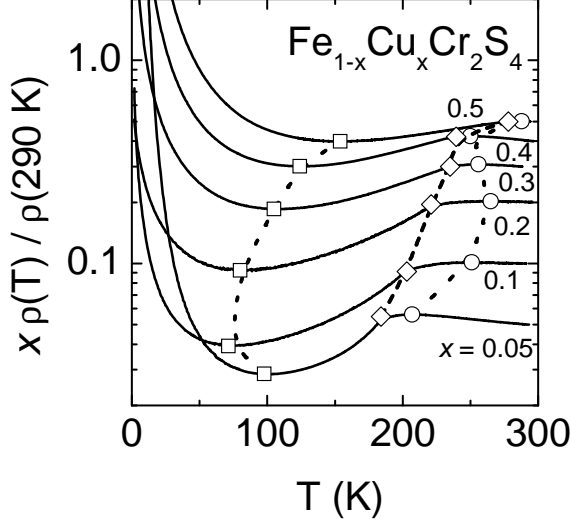
FIG. 4: Electrical Resistivity of $Fe_{1-x}Cu_xCr_2S_4$ normalized at $T = 290$ K and multiplied with the Cu-concentration x. The Cu concentrations x are indicated in the figure. Additionally the Curie temperatures T_C ($\diamond$, dashed line) and the positions of the local minima ($\square$, dotted line) and maxima ($\circ$, dotted line) are given. The current was applied along the $\langle 110 \rangle$-direction.

$$\frac{\nu}{\gamma} = H_{res}^{100} + 2H_A,$$

$$\frac{\nu}{\gamma} = H_{res}^{111} - \frac{4}{3}H_A. \tag{1}$$

Hence, the resonance shift $H_{res} - \nu/\gamma$ from the Larmor frequency is proportional to the anisotropy field. For $H||\langle 100 \rangle$ the shift is negative and the resonance disappears at zero field. However, the shift is positive for $H||\langle 111 \rangle$ and can be followed down to lowest temperatures, only limited by the field range, which is accessible to the electromagnet. For this reason we can directly compare the temperature dependence of the anisotropy field calculated from the magnetization measurements for $x = 0.05$ (inset of figure 2) with the temperature dependence of the FMR shift and use the results from FMR to determine the anisotropy field for all Cu concentrations. This clearly indicates the continuous decrease of the magnetic anisotropy with increasing Cu concentration.

D. Electrical Resistivity

Figure 4 shows a semi-logarithmic plot of the resistivity of $Fe_{1-x}Cu_xCr_2S_4$ normalized by the room-temperature resistivity and multiplied with the Cu concentrations $x = 0.05, 0.1, 0.2, 0.3, 0.4,$ and 0.5, to enable the identification of the different concentrations. The absolute
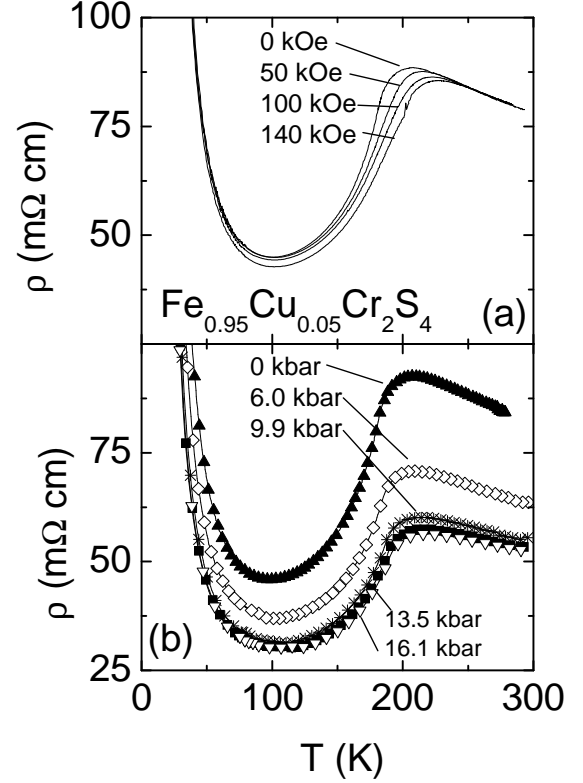

FIG. 5: (a) Resistivity of $Fe_{0.95}Cu_{0.05}Cr_2S_4$ near T_C in magnetic fields up to 140 kOe. The magnetic field is applied in $\langle 111 \rangle$-direction with the current in $\langle 110 \rangle$-direction. (b) Resistivity of $Fe_{0.95}Cu_{0.05}Cr_2S_4$ under hydrostatic pressure.

values of the resistivity at room temperature are summarized in table I. One should keep in mind that such absolute values are given with a large uncertainty. The given error of 10% is the error due to the determination of the geometric factor. A similar order of magnitude and tendency of concentration dependence of the values given here was observed in single crystals by Haacke and Beegle.[27]

The resistivity of $Fe_{1-x}Cu_xCr_2S_4$ ($x \leq 0.5$) exhibits a non-monotonic behavior with a local maximum slightly above and a broad minimum below T_C. The resistivity increases strongly at low temperatures, indicating the insulating ground state of the system. The existence of the local extrema is in agreement with the results in $FeCr_2S_4$.[8,11,21]

The resistivity of $Fe_{0.95}Cu_{0.05}Cr_2S_4$ is plotted in figure 5 (a) for different magnetic fields, 0, 50, 100 and 140 kOe. The magnetic field is applied along the hard axis ($\langle 111 \rangle$-direction), the current is applied in $\langle 110 \rangle$-direction. The maximum in the vicinity of the Curie temperature T_C slightly shifts to higher temperatures, while the minimum remains at a constant temperature with increasing magnetic field. The concentrations $x = 0.1$, 0.2, 0.3, and 0.5 show a similar dependence on magnetic field.

The resistivity of $Fe_{0.95}Cu_{0.05}Cr_2S_4$ was also measured under hydrostatic pressure. In figure 5 (b) the resistivity of $Fe_{0.95}Cu_{0.05}Cr_2S_4$ for different pressures up to 16.1 kbar is shown. Under a pressure of 16.1 kbar the resistivity is reduced by 37 % at room temperature. The minimum as well as the local maximum are shifted to higher temperatures (see figure 9 (b) for T_{max} and $\frac{dT_{max}}{dp}$).

IV. DISCUSSION

A. The ionic picture: Triple exchange model

The system $Fe_{1-x}Cu_xCr_2S_4$ can be divided in two different concentration regimes $0 \leq x \leq 0.5$ and $0.5 < x \leq 1$ with different physical properties. The concentration range $0.5 < x \leq 1$ will be treated in a forthcoming paper.

In the region $x \leq 0.5$ the valences of the ions can be described by the formula

$$Fe_{1-2x}^{2+}Fe_x^{3+}Cu_x^+Cr_2^{3+}S_4^{2-}. \tag{2}$$

This description was already given by Lotgering et al.[14] and Goodenough.[15] As a conduction mechanism Palmer and Greaves proposed a triple-exchange model.[28] In this model the electrical conduction is established via hopping between Fe^{2+} and Fe^{3+}. An illustration is given in figure 6. Fe^{2+} has six $3d$-electrons, where the sixth electron is located in the e_g-band with the spin antiparallel to the spins of the other five electrons of Fe and parallel to the Cr-moments, which define the direction of the magnetization. The single electron in the Fe's spin-up e_g-band hops with an exchange mechanism, similar to the well-known double-exchange,[29] via a p-orbital of the sulphur to Cr, providing an additional electron on the Cr site leading to an intermediate Cr^{2+} state. From there it proceeds via the second S to the Fe^{3+}, changing the valence to Fe^{2+}. Because of its antiparallel alignment to the remaining d-electron spins of the Fe, the spin of the hopping electron is parallel to the spin of the electrons in the Cr $3d$-band.[28]

The observed temperature and magnetic field dependence of the resistivity for $0 < x < 0.5$ can be explained by the triple-exchange model. In the paramagnetic region above T_C semi-conducting behaviour due to thermal activated hopping is observed. At T_C the system enters the magnetically ordered state and the Cr and Fe spins are aligned antiparallel, stimulating the hopping via the triple-exchange mechanism and leading to a positive temperature slope of the resistivity. For the absolute values of the resistivity one would expect a minimum at a Cu concentration $x \approx \frac{1}{3}$, where an equal amount of Fe^{2+} and Fe^{3+} exists. The values for the resistivity given in table I show a broad minimum between $x = 0.1$ and 0.3. This is an indication, that the system cannot be described by an pure ionic picture only. Thus, in the next section a description in a band picture will be given.

The attempts to fit the low-temperature increase of the resistivity with an Arrhenius- ($\rho \propto \exp\left(\frac{T_0}{T}\right)$) or a
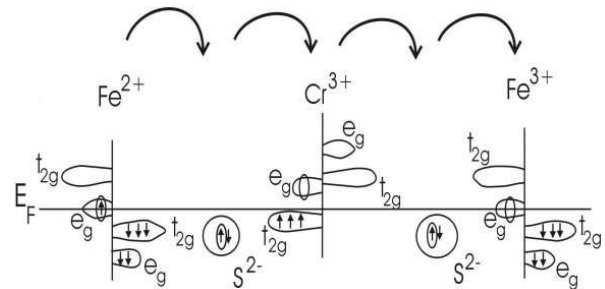

FIG. 6: Illustration of the triple-exchange between Fe^{2+} and Fe^{3+} via S and Cr. The rough position of the bands is adopted from the band structure calculations of Park et al.[30] The mobile electrons and the empty states, into which they are hopping, are circled. For details see text.

variable-range hopping law ($\rho \propto \exp\left(\left(\frac{T_0}{T}\right)^{\frac{1}{4}}\right)$) failed. The rise of the resistivity is weaker than either a simple Arrhenius- or variable-range hopping law and probably cannot be explained by only a single mechanism alone. In the whole temperature regime, variable range hopping is assumed to be the relevant conduction mechanism. But below the ordering temperature the triple exchange enhances the conductivity compared to the simple variable-range hopping process, correlated with the magnetic anisotropy. Also in the ordered phase, there might be additional contributions to the resistivity from magnon scattering which increases with increasing temperature.

B. The band picture: $Fe_{1-x}Cu_xCr_2S_4$ as a half metal

We assume the Fermi-edge to be located within the Fe spin-up e_g-band, as it is shown in figure 6. This assumption is supported by band-calculations of Park et al., who describe $Fe_{1-x}Cu_xCr_2S_4$ as a half-metallic ferromagnet.[30] The half-metallic ferromagnetic state is realized, if all spins are fully polarized forming one metallic and one insulating band.[31] From their calculations Park et al. expected a metallic ground state for $FeCr_2S_4$. The metallic ground state is changed by Coulomb interactions splitting the Fe e_g band, leading to a Mott-insulator.[30] In addition this splitting is supported by the Jahn-Teller effect[32], which is peculiar to Fe^{2+} ions and shown by Mössbauer experiments.[33] At higher temperatures near T_C the thermal activation is high enough to overcome the band splitting, which leads to the observed positive temperature gradient in the resistivity below T_C. Above T_C the spins are not ordered anymore and a simple hopping conductivity is established.

Substituting Fe by Cu empties the Fe^{2+} e_g spin-up band and, thus, destroys the band splitting, which explains the strong decrease of the resistivity in the con-
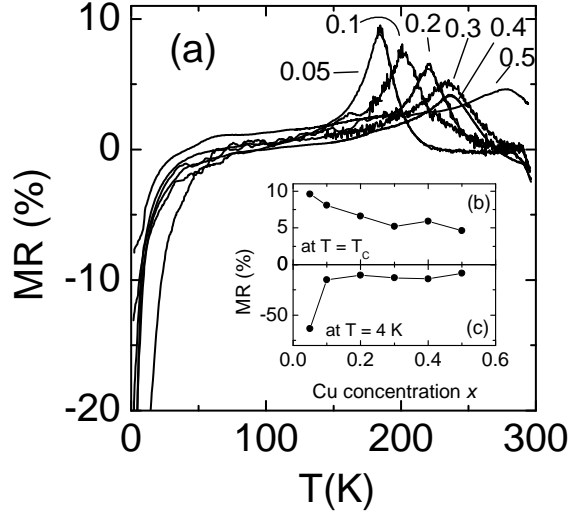
FIG. 7: (a): Magnetoresistance $MR = \frac{\rho(0kOe)-\rho(50kOe)}{\rho(0kOe)}$ of $Fe_{1-x}Cu_xCr_2S_4$ for the concentrations $x = 0.05$, 0.1, 0.2, 0.3 and 0.5. The magnetic field is applied in $\langle 111 \rangle$-direction, the current is applied in the $\langle 110 \rangle$-direction. (b): maximum of the magnetoresistance at the Curie temperature T_C in a magnetic field of $H = 50$ kOe; (c): value of the magnetoresistance at 4 K in a magnetic fields $H = 50$ kOe vs. Cu-concentration x.

centration range up to 10 %. Further substitution of Fe with Cu empties the Fe^{2+} e_g spin-up band, reducing the number of charge carriers and, thus, leads to an eventual increase of the resistivity with increasing x.

At $x = 0.5$ all Fe ions should be trivalent and an insulating ground state is found (although Park *et al.* assume Cu^{2+}).[30] Nevertheless, in the region below T_C a positive temperature gradient of the resistivity is found. To understand this, one has to look on the concentration range $x \geq 0.5$. Here we assume a double-exchange mechanism between Cr^{3+} and Cr^{4+} via S, as proposed by Lotgering *et al.*[34] Slight off-stoichiometries in $Fe_{0.5}Cu_{0.5}Cr_2S_4$ can lead to either that not all Fe^{2+}-ions are changed completely to Fe^{3+} or that already at concentrations $x < 0.5$ Cr^{3+}-ions start to be turned in Cr^{4+} and, thus, give the possibility to process double-exchange in the ordered regime below T_C.

Cu^+ is in $3d^{10}$-state and therefore has a closed d-shell. That is why in the ionic picture Cu is not supposed to contribute to the conductivity. In the band picture the t_{2g}- and e_g-band are completely filled, thus also in this case no contribution to the conductivity is expected.

C. Influence of the magnetic field

The magnetic order is anisotropic due to a strong spin-orbit coupling of the tetrahedral Fe^{2+} ions in the $3d^6$-state.[32,35,36] The 6th d-electron located in the e_g-band (see figure 6) perturbs the symmetry of the charge dis-
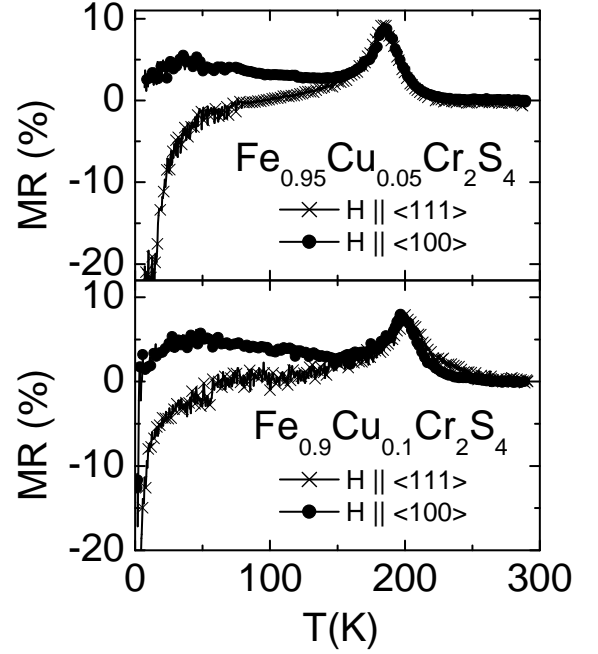

FIG. 8: Magnetoresistance $MR = \frac{\rho(0kOe)-\rho(50kOe)}{\rho(0kOe)}$ of $Fe_{0.95}Cu_{0.05}Cr_2S_4$ (upper frame) and $Fe_{0.9}Cu_{0.1}Cr_2S_4$ with the magnetic field applied along the easy axis $\langle 100 \rangle$ ($\bullet$) and the hard axis $\langle 111 \rangle$ ($\times$). The current was applied in the $\langle 110 \rangle$-direction always.

tribution. This leads to a preferred orientation of the orbitals and with the spin-orbit-coupling to the observed magnetic anisotropy.

In figure 7 (a) the magnetoresistance $MR := \frac{\rho(0kOe)-\rho(50kOe)}{\rho(0kOe)}$ of $Fe_{1-x}Cu_xCr_2S_4$ is displayed. Note, that in our definition $MR > 0$ if $\rho(H) < \rho(0)$. For all concentrations the field was applied along the hard axis $\langle 111 \rangle$. As the magnetic field aligns the spins, the triple-exchange is enhanced and the conductivity grows. This enhancement is most pronounced at T_C due to the onset of spontaneous order and decreases to lower temperatures. At the Curie temperature T_C a peak arises, which was theoretically predicted in metals[37] and is smeared out with increasing Cu-concentration. The maximum of the magnetoresistance vs the Cu-concentration x is drawn in figure 7 (b). It drops from 9.6% at $x = 0.05$ to 4.6% at $x = 0.5$. In the region between 100 and 35 K the magnetoresistance changes its sign and its absolute value grows up to 63% at $T = 4$ K for $x = 0.05$. The values of the magnetoresistance at $T = 4$ K in dependence of the Cu-concentration x are plotted in figure 7 (c). With increasing Cu concentration the magnitude of the magnetoresistance is reduced from 63% at $x = 0.05$ to 8.4% at $x = 0.5$. Using the idea of triple exchange, the last results indicate that obviously the magnetic field, applied along the hard axis, leads to a weak distortion of the e_g-orbital of Fe out of its preferred direction, reducing the overlap between the orbitals that participate in the hop-
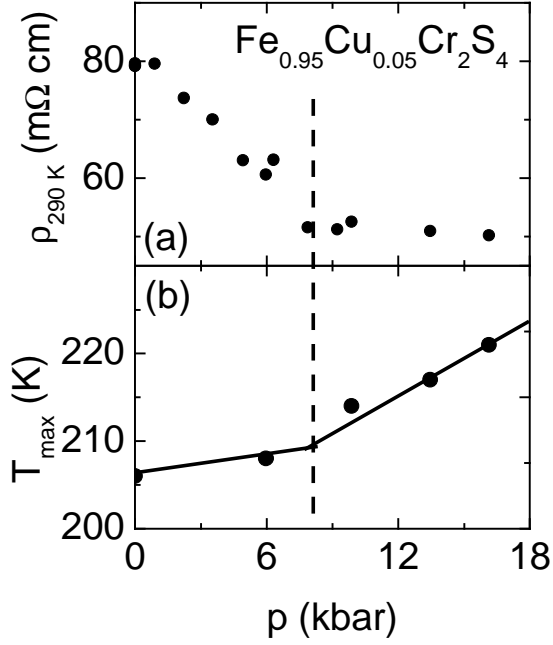
FIG. 9: (a) Resistivity of $Fe_{0.95}Cu_{0.05}Cr_2S_4$ at $T = 290$ K in dependence of the applied hydrostatic pressure. (b) Shift of the local maximum in the resistivity of $Fe_{0.95}Cu_{0.05}Cr_2S_4$, as obtained from figure 5 (b)(closed circles, ●). The dashed line indicates the critical pressure at about $p \approx 8$ kbar.

FIG. 10: Relative change of resistivity under hydrostatic pressure $PR = \frac{\rho(0\text{kbar}) - \rho(p)}{\rho(0\text{kbar})}$.

ping process, and therefore to the observed enhancement of the resistance in a magnetic field.

Applying a magnetic field along the easy axis allows the Fe e_g orbital to remain in its favored direction and so the overlap between the e_g orbital of Fe and the orbital of S is not changed significantly. In this case the magnetoresistance remains positive to lower temperatures, as it is shown in figure 8. There the magnetoresistance of $Fe_{0.95}Cu_{0.05}Cr_2S_4$ and $Fe_{0.9}Cu_{0.1}Cr_2S_4$ is displayed with the magnetic field applied along the easy and along the hard axis. When applying the field along the easy axis, the magnetoresistance exhibits a weak maximum. It changes sign at significantly lower temperatures than upon application of the field along the hard axis only for the sample with Cu concentration $x = 0.1$. This change of sign may result from small misorientations of the sample in the magnetic field, due to the experimental conditions.

D. Influence of hydrostatic pressure

In Ref. 21 was shown that by the application of pressure the Curie temperature T_C is shifted to higher temperatures as indicated by the shift of the temperature of the local maximum T_{max} of the $\rho(T)$ curves. There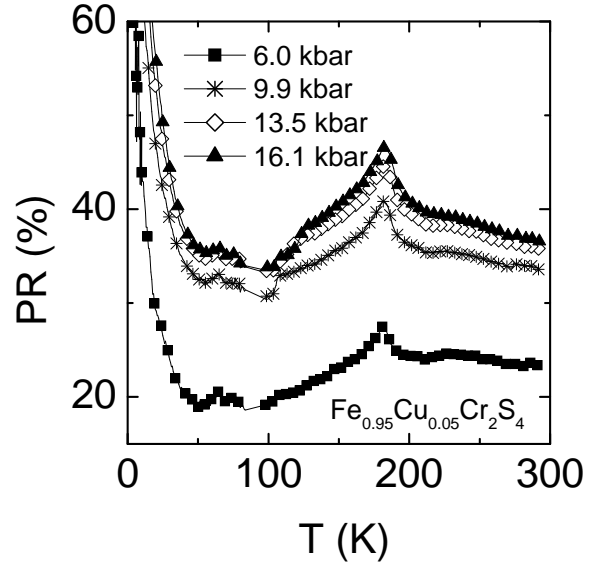fore we conclude that the same effect works for the Cu-doped compounds, and the shift of T_{max} can be taken as the shift of T_C.

The pressure dependence of the resistivity of $Fe_{0.95}Cu_{0.05}Cr_2S_4$ at $T = 290$ K is drawn in figure 9 (a). At a pressure of approximately 8 kbar the resistivity has declined about 37% from its value at ambient pressure. For higher pressures $\rho(290$ K) stays constant. On the other hand, the temperature of the local maximum in the $\rho(T)$ curve (see figure 5 (b)) increases stronger with pressures above 8 kbar, as shown in figure 9 (b). Therefore one can assume that the effect of hydrostatic pressure is changed, when a critical value $p \approx 8$ kbar is exceeded. In contrast to $La_{1-x}Sr_xMnO_3$, where a linear pressure dependence was found,[38] in the present system two different pressure regimes with different pressure gradients in T_{max} are in place.

Figure 10 displays the effect of pressure on the electrical resistance (PR), which is defined in analogy to the magnetoresistance MR as $PR := \frac{\rho(0 \text{ kbar}) - \rho(p)}{\rho(0 \text{ kbar})}$. There are two remarkable features: first of all, at the Curie temperature T_C a peak, similar to the magnetoresistance, arises, however, second the value of PR does not change sign at low temperatures and its absolute value increases up to 100 %.

The application of hydrostatic pressure is expected to increase the overlap between the orbitals and to broaden the bands, resulting in an enhanced mobility of the charge carriers and a reduction of the energy gap between the bands. This yields an enhanced electric conductivity, which is illustrated in figure 10. Similar behavior was found in manganites, for example in polycrystalline $La_{1-x}Ca_xMnO_3$.[39] If one would approximately describe the different conducting mechanisms with different hop-

ping laws, a reduction of the hopping barriers automatically yields the strong increase of the PR value at low temperatures. However, it is necessary to bear in mind that the pressure is relatively moderate in the present study. Thus its effect on the hopping barriers is not expected to be such large and one has to look for an other mechanism. For example the pressure might affect the Jahn-Teller distortion and this way reinforce the conductivity.

V. CONCLUSION

In this paper X-ray, magnetization, FMR and resistivity data from single crystals of $Fe_{1-x}Cu_xCr_2S_4$ are presented. The results are discussed in a hopping model, where the conductivity is explained by triple-exchange mechanisms for the concentration range $x < 0.5$ and double-exchange for $x \geq 0.5$.

Applying an external magnetic field or hydrostatic pressure to the system ($x \leq 0.5$) has qualitatively an analogous effect for temperatures around the Curie temperature T_C: the overlap of the orbitals is enhanced and the bands are broadened. Thus the conductivity increases, while T_C is shifted upward. At lower temperatures this similarity of the effect of an external magnetic field and hydrostatic pressure vanishes. While the value of PR shows a strong upturn at low temperatures, in the magnetoresistance a strong anisotropy arises. Applying the magnetic field along the hard axis leads to a strong negative magnetoresistance, while applying the field along the easy axis results in a flat maximum in the magnetoresistance. Since the origin of this unusual feature is still unclear, further investigations of the electronic and orbital correlations in $Fe_{1-x}Cu_xCr_2S_4$ are needed and a promising challenge for future experiments and theoretical calculations.

[1] G. Jonker and J. H. van Santen, Physica **16**, 337 (1950).

[2] J. H. van Santen and G. Jonker, Physica **16**, 599 (1950).

[3] R. von Helmolt, J. Wecker, B. Holzapfel, L. Schultz, and K. Samwer, Phys. Rev. Lett. **71**, 2331 (1993).

[4] C. W. Searle and S. T. Wang, Can. J. Phys. **48**, 2023 (1970).

[5] A. J. Millis, P. B. Littlewood, and B. I. Shraiman, Phys. Rev. Lett. **74**, 5144 (1995).

[6] M. B. Salamon and J. Marcelo, Rev. Mod. Phys. **73**, 583 (2001).

[7] A. P. Ramirez, J. Phys.: Condens. Matter **9**, 8171 (1997).

[8] T. Watanabe, Solid State Commun. **12**, 355 (1973).

[9] K. Ando, Y. Nishihara, T. Okuda, and T. Tsushima, J. Appl. Phys. **50**, 1917 (1979).

[10] R. P. van Stapele, in *Ferromagnetic Materials* (North-Holland Publishing Company, 1982), vol. 3, pp. 603–745.

[11] A. P. Ramirez, R. J. Cava, and J. Krajewski, Nature **386**, 156 (1997).

[12] G. Haacke and L. C. Beegle, J. Phys. Chem. Solids **28**, 1699 (1967).

[13] H. Hahn, C. de Lorent, and B. Harder, Z. Anorg. Chem. **283**, 138 (1956).

[14] F. K. Lotgering, R. P. van Stapele, G. H. A. M. van der Steen, and J. S. van Wieringen, J. Phys. Chem. Solids **30**, 799 (1969).

[15] J. B. Goodenough, J. Phys. Chem. Solids **30**, 261 (1969).

[16] G. Haacke and A. J. Noizik, J. Solid State Commun. **6**, 363 (1968).

[17] Z. Chen, S. Tan, Y. Zhaorong, and Y. Zhang, Phys. Rev. B **59**, 11172 (1999).

[18] V. Tsurkan, M. Demeter, B. Schneider, D. Hartmann, and M. Neumann, Solid State Commnun. **114**, 149 (2000).

[19] J. Matsuno, T. Mizokawa, A. Fujimori, D. A. Zatsepin, V. R. Galakhov, E. Z. Kurmaev, Y. Kato, and S. Nagata, Phys. Rev. B **55**, R15979 (1997).

[20] P. G. Radaelli, Y. Horibe, M. J. Gutmann, H. Ishibashi, C. H. Chen, R. M. Ibberson, Y. Koyama, Y.-S. Hor, V. Kiryukhin, and S.-W. Cheong, Nature **416**, 155 (2002).

[21] V. Tsurkan, I. Fita, M. Baran, R. Puzniak, R. Szymczak, H. Szymczak, S. Klimm, M. Klemm, S. Horn, and R. Tidecks, J. Appl. Phys. **90**, 875 (2001).

[22] A. Arrott, J. Appl. Phys. **42**, 1282 (1971).

[23] V. Tsurkan, M. Lohmann, H.-A. Krug von Nidda, A. Loidl, S. Horn, and R. Tidecks, Phys. Rev. B **63**, 125209 (2001).

[24] C. Kittel, Phys. Rev. **71**, 270 (1947).

[25] C. Kittel, Phys. Rev. **73**, 155 (1948).

[26] A. G. Gurevich and G. A. Melkov, *Magnetization Oscillations and Waves* (CRC Press, Boca Raton, FL, 1996).

[27] G. Haacke and L. C. Beegle, J. Appl. Phys. **39**, 656 (1968).

[28] H. M. Palmer and C. Greaves, J. Mater. Chem. **9**, 637 (1999).

[29] C. Zener and R. R. Heikes, Rev. Mod. Phys. **25**, 191 (1953).

[30] M. S. Park, S. K. Kwon, S. J. Youn, and B. I. Min, Phys. Rev. B **59**, 10 018 (1999).

[31] R. A. de Groot, F. M. Mueller, P. G. van Engen, and K. H. J. Buschow, Phys. Rev. Lett. **50**, 2024 (1983).

[32] L. F. Feiner, J. Phys. C: Solid State Phys. **15**, 1515 (1982).

[33] M. R. Spender and A. H. Morrish, Solid State Commun. **11**, 1417 (1972).

[34] F. K. Lotgering, Solid State Commun. **2**, 55 (1964).

[35] B. Hoekstra, R. P. van Stapele, and A. B. Voermans, Phys. Rev. B **6**, 2762 (1972).

[36] L. Goldstein, P. Gibart, and L. Brossard, in *AIP Conf. Proc.* (1976), vol. 29, pp. 405–407.

[37] I. A. Campbell and A. Fert, in *Ferromagnetic Materials*

(North-Holland Publishing Company, 1982), vol. 3, pp. 747–804.

[38] Y. Moritomo, A. Asamitsu, and Y. Tokura, Phys. Rev. B **51**, 16491 (1995).

[39] J. J. Neumeier, M. F. Hundley, J. D. Thompson, and R. H. Heffner, Phys. Rev. B **52**, R7006 (1995).